Hole U1415H[1]

K.M. Gillis, J.E. Snow, A. Klaus, G. Guerin, N. Abe, N. Akizawa, G. Ceuleneer, M.J. Cheadle, Á. Adrião, K. Faak, T.J. Falloon, S.A. Friedman, M.M. Godard, Y. Harigane, A.J. Horst, T. Hoshide, B. Ildefonse, M.M. Jean, B.E. John, J.H. Koepke, S. Machi, J. Maeda, N.E. Marks, A.M. McCaig, R. Meyer, A. Morris, T. Nozaka, M. Python, A. Saha, and R.P. Wintsch[2]

Chapter contents

[1] Gillis, K.M., Snow, J.E., Klaus, A., Guerin, G., Abe, N., Akizawa, N., Ceuleneer, G., Cheadle, M.J., Adrião, Á., Faak, K., Falloon, T.J., Friedman, S.A., Godard, M.M., Harigane, Y., Horst, A.J., Hoshide, T., Ildefonse, B., Jean, M.M., John, B.E., Koepke, J.H., Machi, S., Maeda, J., Marks, N.E., McCaig, A.M., Meyer, R., Morris, A., Nozaka, T., Python, M., Saha, A., and Wintsch, R.P., 2014. Hole U1415H. *In* Gillis, K.M., Snow, J.E., Klaus, A., and the Expedition 345 Scientists, *Proc. IODP,* 345: College Station, TX (Integrated Ocean Drilling Program). doi:10.2204/iodp.proc.345.108.2014
[2] **Expedition 345 Scientists' addresses.**

Operations

The location of Integrated Ocean Drilling Program Hole U1415H (see Fig. **F8** in the "Expedition 345 summary" chapter [Expedition 345 Scientists, 2014b]) was selected to test sediment thickness and subseafloor drilling conditions, with the aim of finding a suitable site for establishing a deep hole. Hole operations are summarized in Table **T1** and outlined below. All times are ship local time (UTC – 7 h).

Near-bottom 3.5 kHz pinger and camera survey

At the end of operations in Hole U1415G and while still at that location, we lowered the camera system with the 3.5 kHz pinger attached and conducted a new survey of the seafloor and near-subbottom (see Table **T1** and Fig. **F3** in the "Bench site survey" chapter [Expedition 345 Scientists, 2014a]) en route to Hole U1415H, located 20 m west and 15 m south of Hole U1415G.

Drilling operations

After arriving at the coordinates for Hole U1415H, we visually observed the drill bit tag the seafloor at 4857.6 meters below rig floor (mbrf). The camera system was recovered, and Hole U1415H was spudded at 1040 h on 27 December 2012. Rotation began after penetrating ~1.0 m of soft material, and rotary core barrel coring continued to 12.9 meters below seafloor (mbsf). Core 345-U1415H-1R recovered 0.44 m (3% recovery). Drilling conditions in this hole were vastly different than in previous holes. All drilling parameters were much smoother and less erratic; however, when preparing to make a connection, the driller raised the bit off bottom. When the driller attempted to lower the bit back to bottom, immediate formation resistance was encountered. Drilling torque became elevated and erratic, indicating that the hole had once again fallen in. Because it was considered unsafe to attempt making a connection under these circumstances, the decision was made to terminate the hole before possible loss or damage to another bottom-hole assembly. The bit was pulled clear of the seafloor at 0410 h on 28 December, ending Hole U1415H.

Igneous petrology

Coring in Hole U1415H recovered seven different igneous lithologies from 10 intervals from a surficial "rubble" zone, which were

doi:10.2204/iodp.proc.345.108.2014

collectively defined as lithologic Unit I (Fig. F1). Below we give a brief lithologic description for each rock type recovered in the different intervals based on macroscopic and, where available, microscopic observations.

Olivine gabbro

Olivine gabbro defines two intervals (Intervals 9 and 10) in Unit I in Hole U1415H (Thin Section 10; Sample 345-U1415H-1R-1, 51–53 cm [Piece 10]). The olivine gabbro is a medium-grained equigranular granular rock (Fig. F2) that consists of olivine (10%–18%), plagioclase (60%–65%), and clinopyroxene (17%–30%), with trace amounts of oxide. Olivine is fine grained and subhedral to anhedral with an irregular amoeboid habit. Plagioclase is medium grained and subhedral to euhedral with a tabular habit. Clinopyroxene is medium to coarse grained and anhedral with an interstitial to poikilitic habit. In one sample (345-U1415H-1R-1, 51–53 cm [Piece 10]), olivine also forms poikilitic crystals (Fig. F3), a feature that becomes characteristic in gabbro in Hole U1415J.

Olivine-bearing gabbro

Olivine-bearing gabbro defines one lithologic interval (Interval 1). A thin section was cut (Thin Section 7; Sample 345-U1415H-1R-1, 0–4 cm [Piece 1]) for microscopic observations. The olivine-bearing gabbro is medium-grained equigranular granular rock that is moderately to highly altered. Modally, the olivine-bearing gabbro consists of olivine (2%), plagioclase (60%), and clinopyroxene (38%). Olivine is fine grained and subhedral to euhedral with a subequant habit. Plagioclase is medium grained and subhedral to euhedral with a tabular habit. Clinopyroxene is medium grained and anhedral with an interstitial habit.

Orthopyroxene-bearing olivine gabbro

Orthopyroxene-bearing olivine gabbro defines two intervals (Intervals 3 and 8). In general, orthopyroxene-bearing olivine gabbro is medium-grained equigranular granular rock. Interval 3 is foliated. Modally, orthopyroxene-bearing olivine gabbro consists of olivine (6%–7%), plagioclase (70%), clinopyroxene (20%), and orthopyroxene (4%), with trace amounts of oxide. Olivine is fine grained and euhedral to anhedral with a subequant habit. Plagioclase is medium grained and euhedral to subhedral with a tabular habit. Clinopyroxene is medium to coarse grained and subhedral to anhedral with an interstitial to oikocrystic habit. Orthopyroxene is euhedral to subhedral with a prismatic habit.

Gabbro

Gabbro defines two intervals (Intervals 5 and 6) and is a medium-grained equigranular (Interval 5) or seriate poikilitic (Interval 6) granular rock. Modally, gabbro consists of plagioclase (50%–70%) and clinopyroxene (30%–50%), with trace amounts of olivine and oxide. Plagioclase is fine grained and subhedral to euhedral with a tabular habit. Clinopyroxene is medium to coarse grained and anhedral with an interstitial to oikocrystic habit.

Orthopyroxene-bearing gabbro

Orthopyroxene-bearing gabbro defines one interval (Interval 7). A thin section was cut (Thin Section 9; Sample 345-U1415H-1R-1, 33–36 cm [Piece 7]) for microscopic observations. Orthopyroxene-bearing gabbro is medium-grained inequigranular ophitic rock. Modally, orthopyroxene-bearing gabbro consists of plagioclase (50%), clinopyroxene (44%), orthopyroxene (4%), and olivine (2%). Plagioclase is medium grained and subhedral with a tabular habit. Clinopyroxene is anhedral with an irregular to subophitic habit. Orthopyroxene is subhedral to subhedral with a prismatic habit.

Olivine-bearing gabbronorite

Olivine-bearing gabbronorite defines one interval (Interval 4). A thin section was cut (Thin Section 8; Sample 345-U1415H-1R-1, 18–22 cm [Piece 4]) for microscopic observations. Olivine-bearing gabbronorite is medium-grained equigranular granular rock (Fig. F4). Modally, the olivine-bearing gabbronorite consists of olivine (3%), plagioclase (50%), clinopyroxene (35%), and orthopyroxene (12%), with trace amounts of oxide. Olivine is fine grained and anhedral with an irregular amoeboid habit. Plagioclase is medium grained and subhedral to euhedral with a tabular habit, showing a marked zoning in part exhibiting ghostly indistinct zonation (Fig. F5). Clinopyroxene is medium grained and euhedral to subhedral with a tabular to oikocrystic habit. Orthopyroxene is subhedral to euhedral with a subequant habit.

Anorthosite

Anorthosite comprised one interval (Interval 2). The rock is coarse grained and granular with a seriate grain size distribution. Plagioclase comprises 100% of the rock and is euhedral to subhedral with a tabu-

lar habit. Trace amounts of orthopyroxene and oxide are present.

Metamorphic petrology

Background alteration

The lithologies recovered in Hole U1415H consist mainly of relatively unaltered olivine gabbro and olivine gabbronorite. Samples exhibit metamorphism over a wide range of grades and intensities, but because they are from a rubble unit, no patterns of alteration can be established. Primary mineral replacement ranges from 10% to >90%; the typical range is 10%–30%. Pyroxene is slightly to moderately altered to pale green amphibole, and olivine is strongly replaced by serpentine with mesh textures. Corona textures are developed in some of the pieces. Clinopyroxene and orthopyroxene are altered to poorly crystalline green amphibole. In most of the lithologies, plagioclase is slightly altered (typically <10%) to prehnite and secondary plagioclase. Plagioclase is replaced by chlorite where it contacts relict olivine along microfractures. A number of the pieces from this core appear to be from cataclastic zones (see **"Structural geology"**), with intense fracturing of minerals and enhanced alteration of plagioclase to prehnite and zeolites. Cataclastic cements include zeolites, prehnite, and clay minerals; this assemblage appears to replace fine-grained cataclastic material in some cases (Fig. **F6**). Zeolites identified by X-ray diffraction include thomsonite and chabazite (Table **T2**).

Veins

Veins are composed of several mineralogies, including monomineralic pale green amphibole, prehnite, and clay minerals, as well as amphibole-prehnite, amphibole-clay minerals, and amphibole-secondary plagioclase. Pieces in this core typically have one or two thin (<1–2 mm wide), isolated veins. Vein shapes range from regular to anastomosing single veins to relatively dense networks of thin veins (e.g., Sample 345-U1415H-1R-1 [Piece 7]). Halos are 1–3 mm thick and are characterized by more complete alteration of mafic minerals, particularly olivine to serpentine, and enhanced alteration of plagioclase to chlorite.

Metamorphic conditions

The alteration observed in these samples is variable, as would be expected in rocks from discontinuous intervals. The dominant alteration of all recovered rocks is greenschist to zeolite facies. The alteration predominantly affects pyroxene and olivine, except in cataclastic zones where prehnite, secondary plagioclase, and zeolite pervasively replace plagioclase.

Structural geology

All core pieces from Hole U1415H were relatively small (8 cm maximum length), not cored or oriented, and likely from loose rubble that comprises lithologic Unit I.

Magmatic structures

Samples recovered from Hole U1415H show no magmatic layering. One piece of olivine gabbronorite (Sample 345-U1415H-1R-1, 18–22 cm [Piece 4]) exhibits weak plagioclase and pyroxene shape-preferred orientation (SPO) (Fig. **F7A**), and four pieces of olivine gabbro (Sample 1R-1 [Pieces 3, 8, 9, and 10]) (Fig. **F7B**) exhibit planar, weak to moderate plagioclase and olivine SPO. The olivine gabbro is similar to Pieces 1 and 3 in Section 345-U1415G-1R-1. Most medium-grained pieces that were cut and large enough show magmatic foliation; however, the core sample of the partially altered, coarse-grained olivine gabbro (Piece 1) and the altered gabbro (Piece 7) may not be large enough to reveal weak SPO. More than 70% of the core has magmatic foliation.

Microscopic observations show that magmatic foliation is defined by both the preferred orientation and shape anisotropy of plagioclase crystals. The plagioclase crystals are often tabular and 1–4 mm in length, with aspect ratios as high as 4:1 and traces of [010] albite twin planes parallel to the long axes of the crystals. An olivine gabbronorite (Sample 345-U1415H-1R-1, 18–22 cm [Piece 4]) exhibits weak magmatic foliation defined by the SPO of plagioclase and pyroxene (Fig. **F7A**). Plagioclase crystals show gently curved grain boundaries with 120° grain junctions and very rare deformation twins and/or bent grains.

An olivine gabbro (Sample 345-U1415H-1R-1, 51–53 cm [Piece 10]) has moderate and parallel plagioclase SPO, clinopyroxene SPO, and olivine SPO (Fig. **F7B**). The olivine SPO is defined by sometimes tabular, partially skeletal olivine crystals that show minor undulose extinction and subgrain development (Fig. **F7C**). Plagioclase commonly shows deformation twinning (Fig. **F7B–F7E**), occasionally with subgrain development (Fig. **F7D**). Annealed plagioclase grain boundaries are common, with some regions of the sample developing equilibrated clusters of polygonal plagioclase with 120° grain junctions (Fig. **F7E**). Some of the plagioclase crystals show seriate bulging grain boundaries indicative of grain boundary migration (Fig. **F7F**). Locally, clinopyroxene crystals appear to be partially interstitial to the plagioclase and

olivine crystals and thus form SPO. Again, the crystal-plastic deformation likely occurred under hypersolidus conditions during mush formation.

Crystal-plastic deformation

No structurally continuous subsolidus crystal-plastic deformation is observed in the recovered section except for one thin zone (3 mm thick) of protomylonitic deformation along one side of Sample 345-U1415H-1R-1, 0–8 cm (Piece 1).

Cataclastic deformation

Two types of brittle deformation are recognized in Hole U1415H: (1) cohesive cataclasites with associated alteration and veining (Fig. F8) and (2) diffuse fracturing with no vein fill or alteration.

Brittle deformation associated with cohesive cataclasite was identified in several pieces (Sample 345-U1415H-1R-1 [Pieces 1, 3, and 8]) that show localized cataclastic deformation with intensity from moderate to well developed. Although fracturing and/or brecciation is noted throughout each deformed gabbro piece, microstructural observations illustrate strain localization into areas with dense anastomosing fractures and incipient brecciation/cataclasis, overprinted by thin zones of cataclasite (or ultracataclasite) (Fig. F8D, F8E). Locally, these zones involve deformation of prehnite (and/or zeolite) veins in Sample 345-U1415H-1R-1, 33–36 cm (Piece 7) (Fig. F9), suggesting synchronous cracking/cataclasis, low-temperature vein formation, and cataclasis of these newly formed "weak" minerals.

Diffuse fracturing of many recovered pieces, showing only open fractures (i.e., no vein fill or alteration), implies a second period of brittle deformation.

Alteration veins

Alteration veins are present in 6 of the 12 pieces recovered in Hole U1415H (~50% of the pieces). Veins are generally rare (less than a few veins per 10 cm of recovery), with only one piece characterized by a high density of tiny veins forming an anastomosing network. Alteration veins are all very thin (<0.1 cm maximum thickness, in most cases <0.05 cm) and together represent <1% of the core volume. Vein lengths generally exceed the width of the cores (6 cm), although vein terminations (vein tips) are frequently observed; their contact with the host gabbroic rocks is generally clear cut (no alteration halo).

Most of the veins are curved and crosscut each other, showing no preferred orientation at piece scale. Because most pieces are not oriented, no orientation data were collected.

In thin section, the same mineral assemblages (varying combinations of amphibole, chlorite, serpentine, zoisite, prehnite, zeolite, serpentine, and clay) are observed as alteration vein-filling material and as "secondary" material where pervasive replacement of primary igneous minerals (plagioclase, olivine, and pyroxene) occurs in the rock (see **"Metamorphic petrology"**). Alteration veins cut primary igneous minerals that are, as a rule, much thicker than the width of individual veins. Undeformed veins are more common than cataclastic/deformed veins. In some veins, alteration minerals have an isotropic shape (mosaic textures), whereas in others, alteration minerals (usually prehnite) are fibrous, with the orientation of the fibers typically perpendicular to the vein walls.

Temporal evolution

Temporal evolution of structures recovered in Hole U1415H is, from oldest to youngest,

- Intrusion of gabbroic and anorthositic rocks,
- Formation of magmatic fabric (foliation),
- Limited crystal-plastic deformation in the mush and annealing of plagioclase,
- Cataclasis associated with low-temperature faulting and low-temperature vein formation, and
- Open fractures.

Details specific to structural features were illustrated with comments in STRUCTUR in **"Supplementary material."**

Inorganic geochemistry

One olivine-bearing gabbronorite was selected in Hole U1415H (Sample 345-U1415H-1R-1, 17–23 cm) for geochemical analysis. Sample selection was based on discussion among representatives from all expertise groups within the shipboard scientific party. Inductively coupled plasma–atomic emission spectroscopy (ICP-AES) was used for determining major and trace element concentrations, and gas chromatography was used for S, H_2O, and CO_2 quantifications. Results are reported in Table T1 in the "Geochemistry summary" chapter (Expedition 345 Scientists, 2014c). Major and trace elements are reported on a volatile-free basis.

Sample 345-U1415H-1R-1, 17–23 cm, has a loss on ignition of 1.1 wt%, H_2O of 1.4 wt%, and CO_2 of 0.14 wt%. These values are slightly higher than those reported for the gabbronorite sampled in Hole U1415E (Sample 345-U1415E-1R-1, 44–47 cm); however, thin section descriptions indicate that Hole U1415H olivine-bearing gabbronorite is less altered

(~5% versus 10% for Hole U1415E gabbronorite; see thin section descriptions in **"Core descriptions"**). These higher volatile contents may reflect variations in the alteration products of both samples and, in particular, the complete replacement of primary olivine in Sample 345-U1415H-1R-1, 17–23 cm, by hydrous-rich phases such as serpentine (which contains as much as 13 wt% H_2O stoichiometrically). Alternatively, the higher volatile content may indicate centimeter-scale alteration heterogeneities in the degree of alteration within the Hole U1415H olivine-bearing gabbronorite.

Sample 345-U1415H-1R-1, 17–23 cm, is characterized by a high Mg# (cationic Mg/[Mg + Fe] – all Fe as Fe^{2+}) of 81, high Ni (150 ppm) and Cr (1000 ppm) abundances, and low TiO_2 (0.3 wt%) and Y (5 ppm) content compared to Hole U1415E gabbronorite. These compositions may reflect the presence of olivine in the primary mineral assemblage (see **"Igneous petrology"**), and the high Cr content points toward a petrogenetic link with a relatively primitive melt.

Hole U1415H gabbronorite is significantly less evolved than previously sampled Hess Deep gabbro and gabbronorite (e.g., Gillis, Mével, Allan, et al. 1993; Pedersen et al., 1996; Kirchner and Gillis, 2012) and has compositional similarities with primitive gabbros sampled at Pito Deep (Perk et al., 2007).

Physical properties

The only measured physical properties of cores recovered in Hole U1415H are magnetic susceptibility and color reflectance. These data were acquired using the Section Half Multisensor Logger with a measurement interval of 2 cm. Raw data were uploaded to the LIMS database and subsequently filtered to remove spurious points that correspond to empty intervals in the liner, broken pieces, and pieces that were too small. Filtered data are available in PHYSPROP in **"Supplementary material."** Magnetic susceptibility ranges from ~100 × 10^{-5} to 1660 × 10^{-5} SI. Color reflectance parameters L*, a*, and b* mean values are 34.3 ± 2.15, –0.69 ± 0.49, and 1.20 ± 1.37, respectively.

References

Gillis, K., Mével, C., Allan, J., et al., 1993. *Proc. ODP, Init. Repts.,* 147: College Station, TX (Ocean Drilling Program). **doi:10.2973/odp.proc.ir.147.1993**

Gillis, K.M., Snow, J.E., Klaus, A., Guerin, G., Abe, N., Akizawa, N., Ceuleneer, G., Cheadle, M.J., Adrião, Á., Faak, K., Falloon, T.J., Friedman, S.A., Godard, M.M., Harigane, Y., Horst, A.J., Hoshide, T., Ildefonse, B., Jean, M.M., John, B.E., Koepke, J.H., Machi, S., Maeda, J., Marks, N.E., McCaig, A.M., Meyer, R., Morris, A., Nozaka, T., Python, M., Saha, A., and Wintsch, R.P., 2014a. Bench site survey. *In* Gillis, K.M., Snow, J.E., Klaus, A., and the Expedition 345 Scientists, *Proc. IODP,* 345: College Station, TX (Integrated Ocean Drilling Program). **doi:10.2204/iodp.proc.345.103.2014**

Gillis, K.M., Snow, J.E., Klaus, A., Guerin, G., Abe, N., Akizawa, N., Ceuleneer, G., Cheadle, M.J., Adrião, Á., Faak, K., Falloon, T.J., Friedman, S.A., Godard, M.M., Harigane, Y., Horst, A.J., Hoshide, T., Ildefonse, B., Jean, M.M., John, B.E., Koepke, J.H., Machi, S., Maeda, J., Marks, N.E., McCaig, A.M., Meyer, R., Morris, A., Nozaka, T., Python, M., Saha, A., and Wintsch, R.P., 2014b. Expedition 345 summary. *In* Gillis, K.M., Snow, J.E., Klaus, A., and the Expedition 345 Scientists, *Proc. IODP,* 345: College Station, TX (Integrated Ocean Drilling Program). **doi:10.2204/iodp.proc.345.101.2014**

Gillis, K.M., Snow, J.E., Klaus, A., Guerin, G., Abe, N., Akizawa, N., Ceuleneer, G., Cheadle, M.J., Adrião, Á., Faak, K., Falloon, T.J., Friedman, S.A., Godard, M.M., Harigane, Y., Horst, A.J., Hoshide, T., Ildefonse, B., Jean, M.M., John, B.E., Koepke, J.H., Machi, S., Maeda, J., Marks, N.E., McCaig, A.M., Meyer, R., Morris, A., Nozaka, T., Python, M., Saha, A., and Wintsch, R.P., 2014c. Geochemistry summary. *In* Gillis, K.M., Snow, J.E., Klaus, A., and the Expedition 345 Scientists, *Proc. IODP,* 345: College Station, TX (Integrated Ocean Drilling Program). **doi:10.2204/iodp.proc.345.114.2014**

Kirchner, T.M., and Gillis, K.M., 2012. Mineralogical and strontium isotopic record of hydrothermal processes in the lower ocean crust at and near the East Pacific Rise. *Contrib. Mineral. Petrol.,* 164(1):123–141 **doi:10.1007/s00410-012-0729-5**

Pedersen, R.B., Malpas, J., and Falloon, T., 1996. Petrology and geochemistry of gabbroic and related rocks from Site 894, Hess Deep. *In* Mével, C., Gillis, K.M., Allan, J.F., and Meyer, P.S. (Eds.), *Proc. ODP, Sci. Results,* 147: College Station, TX (Ocean Drilling Program), 3–19. **doi:10.2973/odp.proc.sr.147.001.1996**

Perk, N.W., Coogan, L.A., Karson, J.A., Klein, E.M., and Hanna, H.D., 2007. Petrology and geochemistry of primitive lower oceanic crust from Pito Deep: implications for the accretion of the lower crust at the southern East Pacific Rise. *Contrib. Mineral. Petrol.,* 154(5):575–590. **doi:10.1007/s00410-007-0210-z**

Publication: 12 February 2014
MS 345-108

Figure F1. Rock types recovered from lithologic Unit I in Hole U1415H based on macroscopic descriptions. For clarity, only the principal rock names are shown without modifiers.

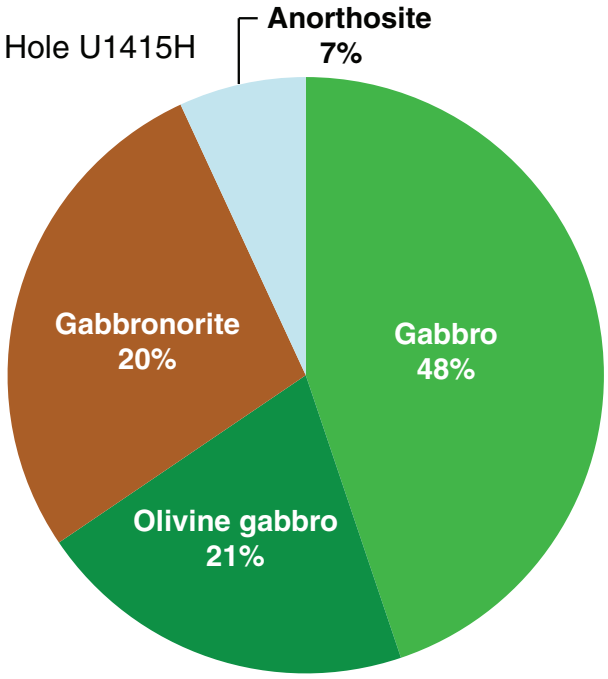

Figure F2. Olivine gabbro (Sample 345-U1415H-1R-1, 48–53 cm [Piece 10]). **A.** Core close-up. **B.** Plane-polarized light. **C.** Under crossed polars.

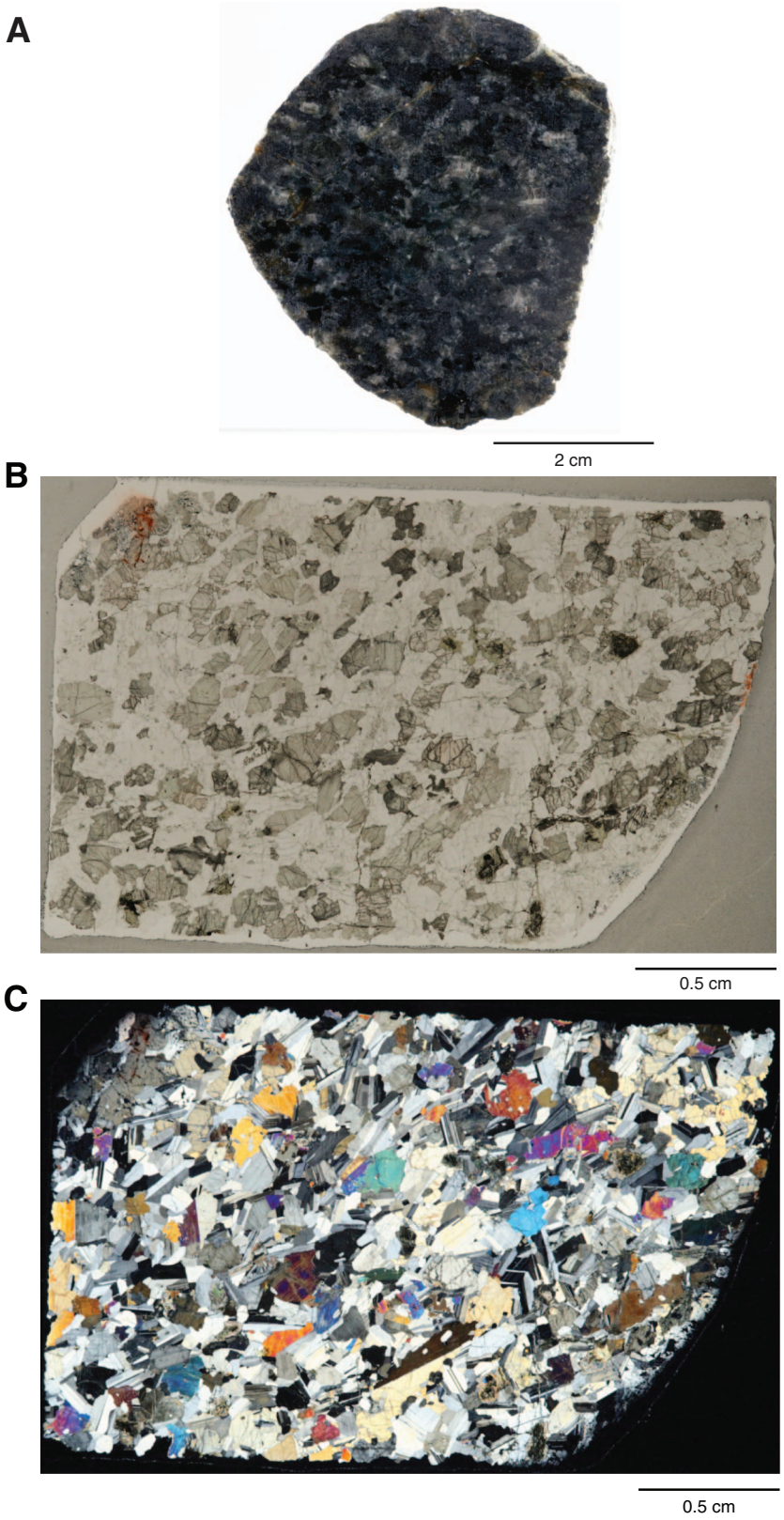

Figure F3. Typical occurrence of anhedral irregularly shaped olivine and anhedral poikilitic clinopyroxene in olivine gabbro (Thin Section 10; Sample 345-U1415H-1R-1, 51–53 cm [Piece 10]). Strong magmatic foliation is indicated by subparallel oriented plagioclase crystals (Pl) and by subparallel alignment of olivine (Ol) and clinopyroxene (Cpx). Note that olivine also shows a tendency to form poikilitic growth. **A.** Plane-polarized light. **B.** Under crossed polars.

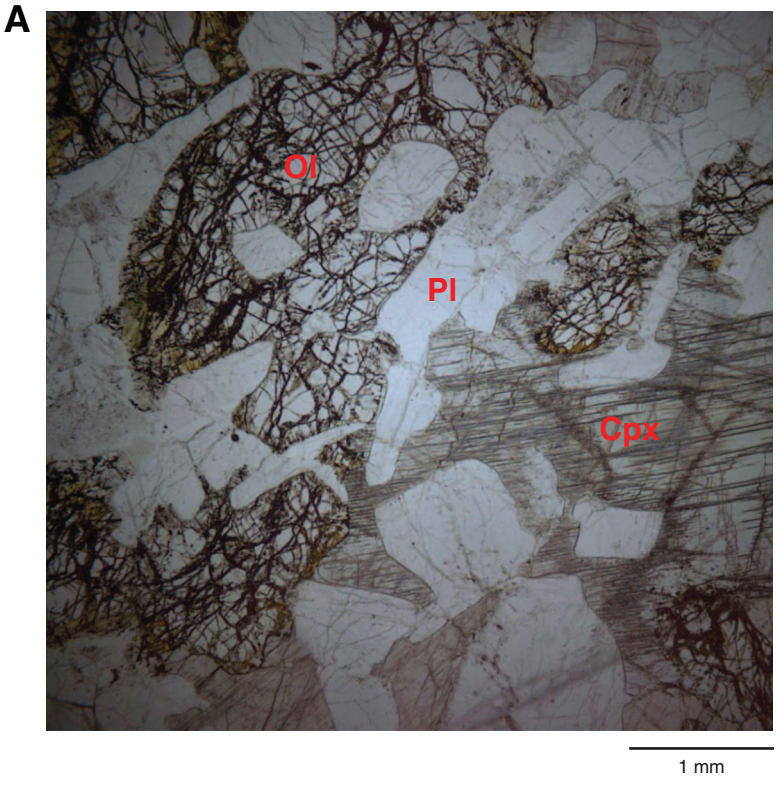

Figure F4. Olivine-bearing gabbronorite (Sample 345-U1415H-1R-1, 18–22 cm [Piece 4]). **A.** Core close-up. **B.** Plane-polarized light. **C.** Under crossed polars.

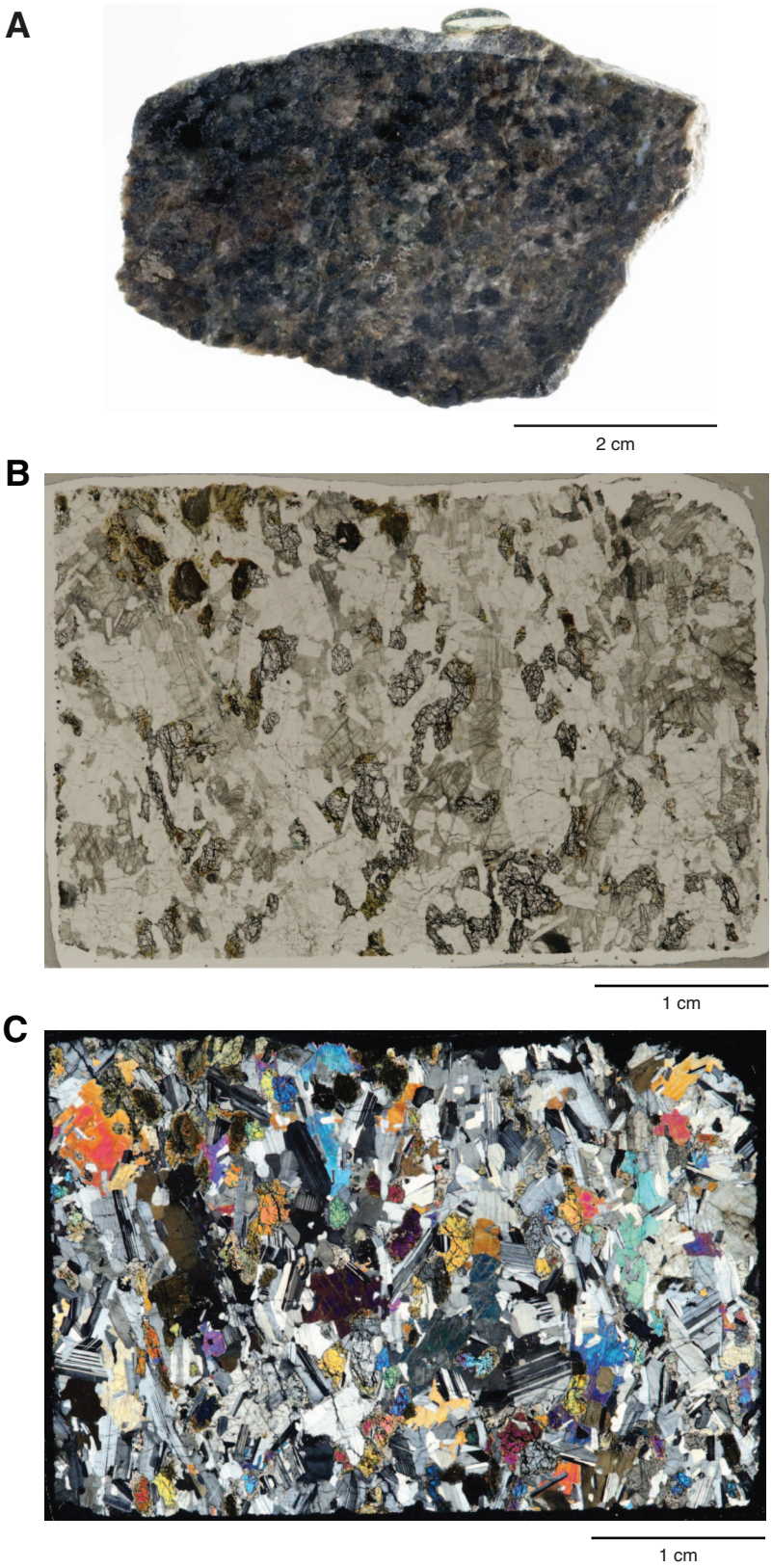

Figure F5. A, B. Zoned plagioclase in olivine-bearing gabbronorite (Thin Section 8; Sample 345-U1415H-1R-1, 18–22 cm [Piece 4]; under crossed polars). Note the presence of indistinct gradational zonation within plagioclase, especially in A, and the well-equilibrated texture with 120° triple junctions between the plagioclase grains. Pl = plagioclase, Cpx = clinopyroxene.

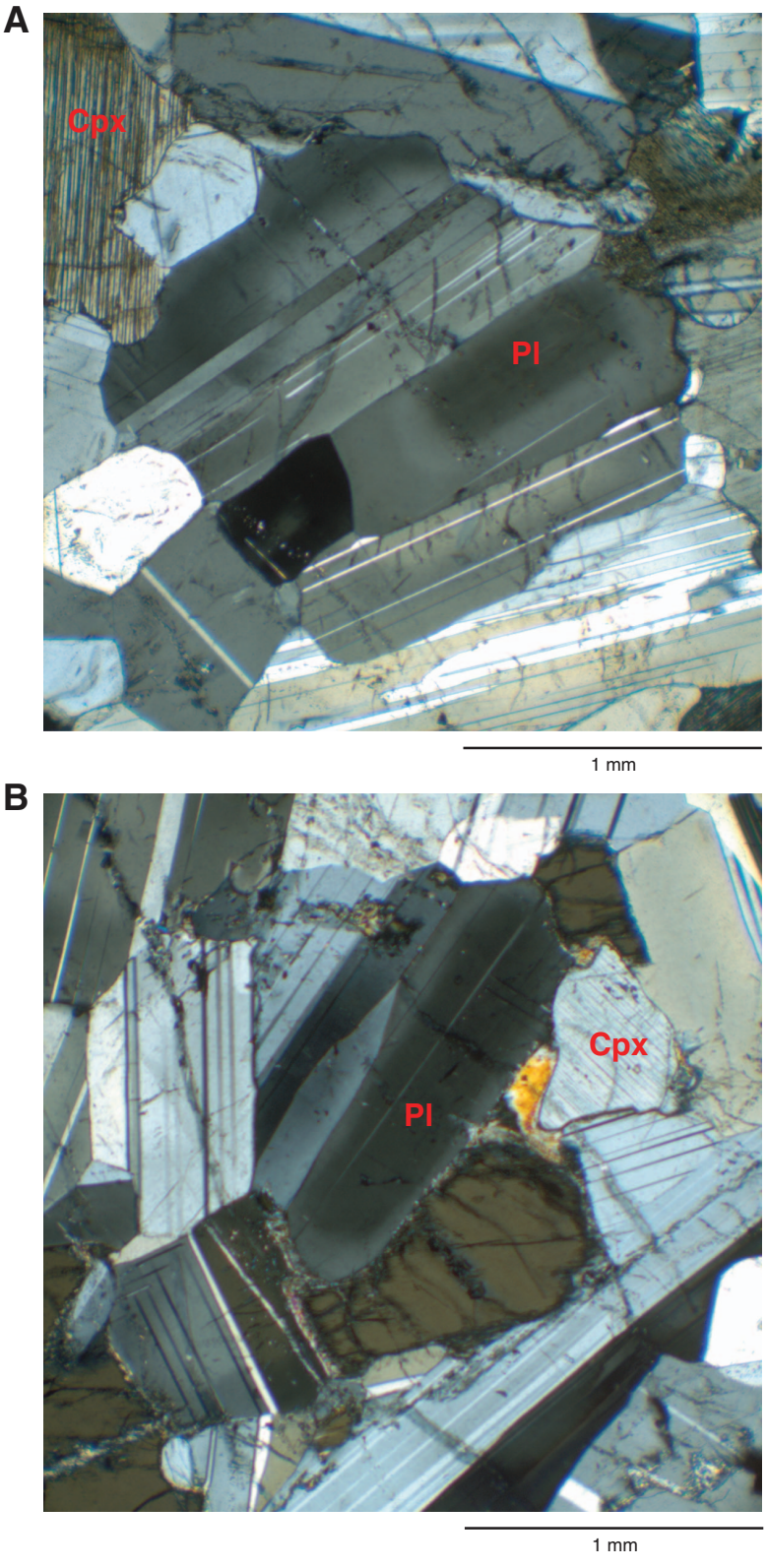

Figure F6. Olivine-gabbro showing a cataclastic zone, also shown in Figure F8 (Thin Section 7; Sample 345-U1415H-1R-1, 0–4 cm [Piece 1]). Clinopyroxene (Cpx) was partially altered to amphibole (Amph) prior to cataclasis, whereas plagioclase (Plag) was partially replaced by zeolite (Ze) after cataclasis. Primary minerals are fractured and cut by a network of zeolite veins. Clasts of pyroxene and amphibole are isolated within zeolite veins. The acute angles of some of these clasts suggest a minimum of replacement prior to cementation by zeolite. **A.** Under crossed polars. **B.** Plane-polarized light.

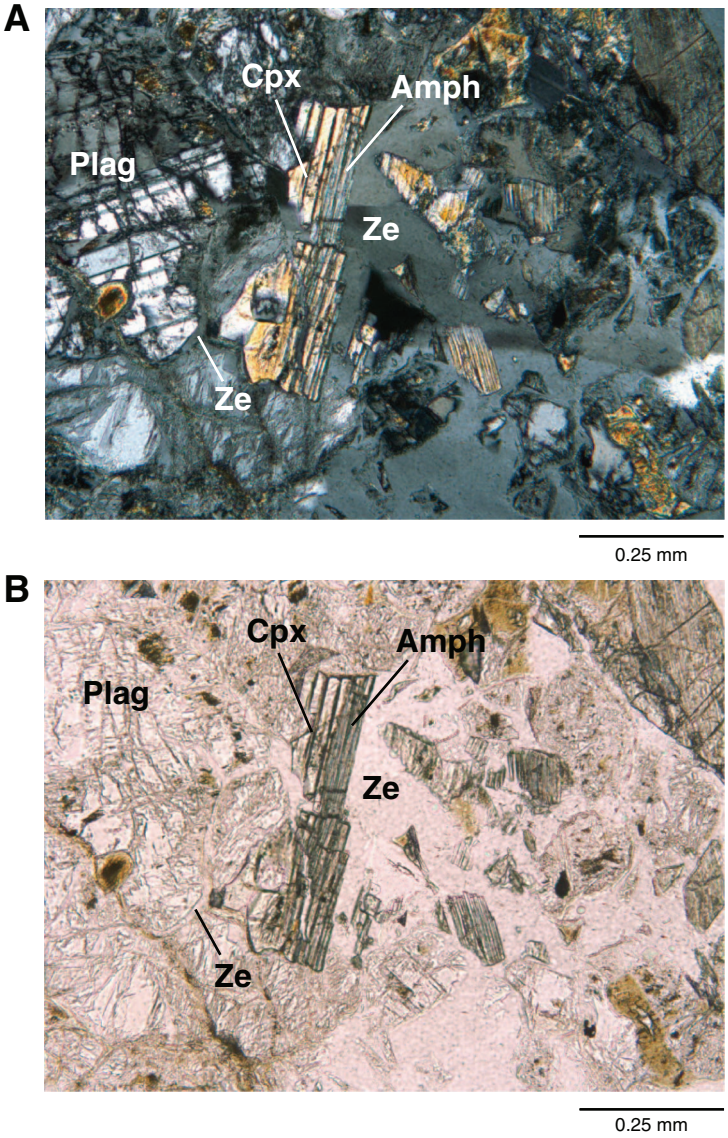

Figure F7. A. Weak plagioclase and pyroxene shape-preferred orientation (SPO; red arrow) (Sample 345-U1415H-1R-1, 18–22 cm [Piece 4]). **B–F.** Sample 345-U1415H-1R-1, 51–53 cm (Piece 10). B. Moderate plagioclase, clinopyroxene, and olivine SPO (red arrow). Olivine SPO is locally defined by tabular, partially skeletal olivine crystals. Red boxes (tick marks show upward direction) indicate location of images in C, E, and F. C. Subgrain development in olivine. D. Deformation twins and subgrain development in plagioclase (this image is outside of the area shown in B). E. Equilibrated cluster of polygonal plagioclase with 120° grain junctions. F. Plagioclase crystals showing seriate, bulging grain boundaries, indicative of grain boundary migration.

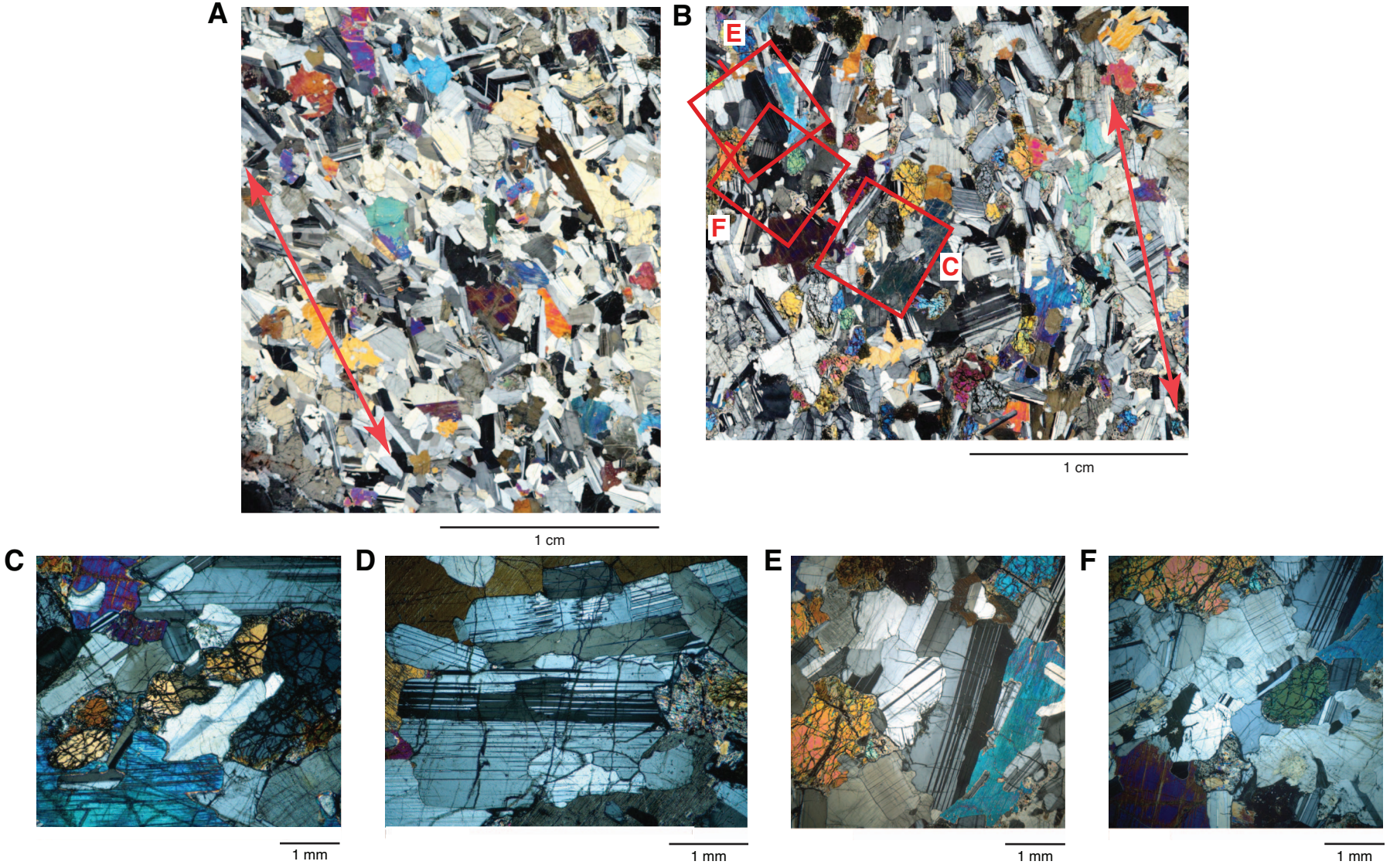

Figure F8. Brittle structures in olivine gabbro (Sample 345-U1415H-1R-1, 0–4 cm [Piece 1]). **A.** Macroscopic character of cataclastic deformation. **B.** Cataclastic deformation along the sample margin. Outlines show the location of C–F. **C.** Localized zone of cataclasite hosting angular clasts in a dark, clay-rich(?) matrix. **D.** Zone of localized strain in cataclasite, small rounded clasts in a clay-filled matrix. **E.** Sharp boundary between zones of moderate-intensity cataclasite and ultracataclasite. **F.** Fractured plagioclase and clinopyroxene crystals occur throughout the thin section, forming cataclastic zones with angular clasts, formed by grain size reduction and grain rotation. B, E, and F are under crossed polars; C and D are under plane-polarized light.

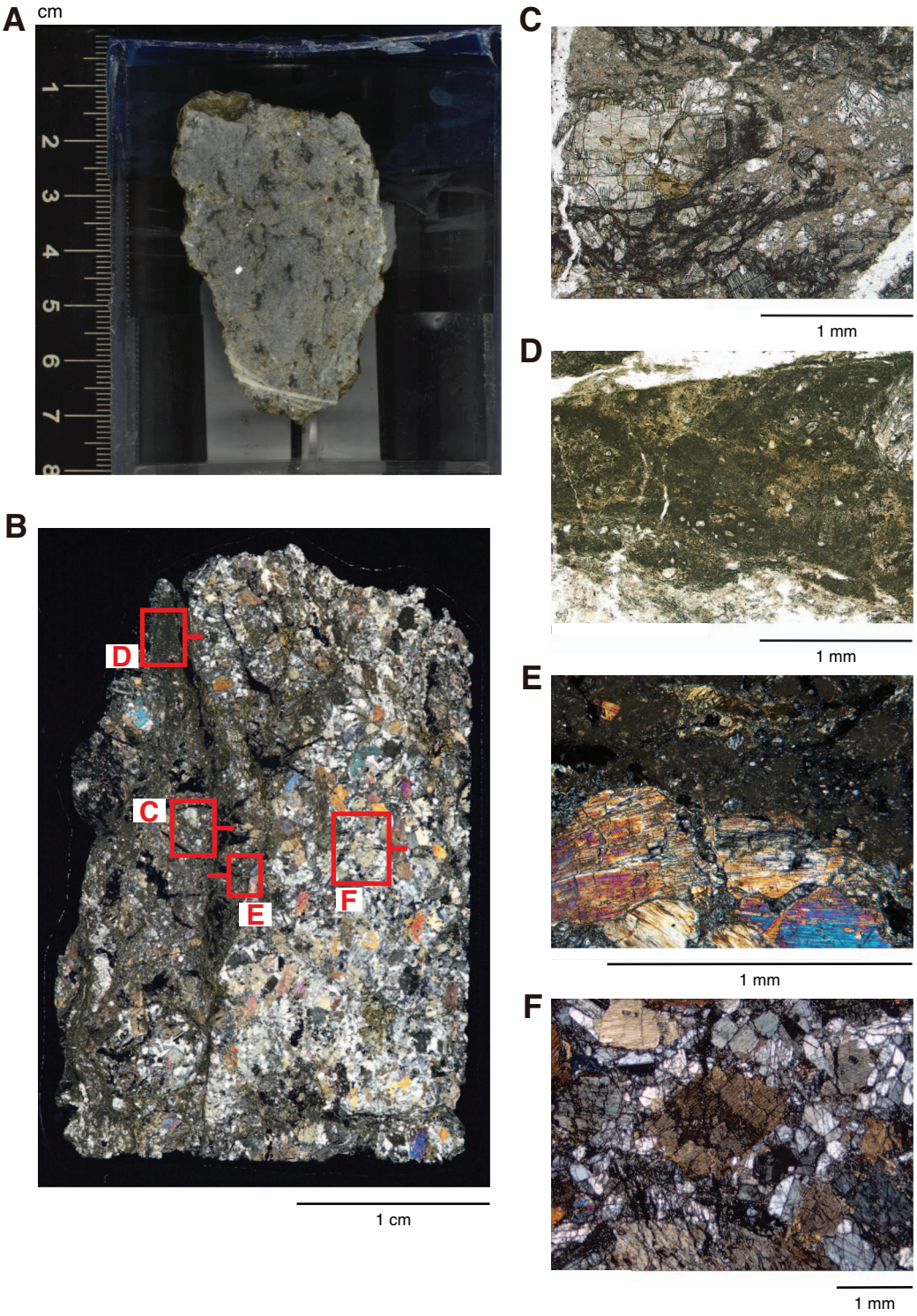

Figure F9. Brittle structures in orthopyroxene-bearing gabbro (Sample 345-U1415H-1R-1, 30–37 cm [Piece 7]; under crossed polars). **A.** Macroscopic character of cataclastic deformation. **B.** Thin section scan showing overview of cataclastic deformation. Red boxes outline locations of images in C–E. **C.** Fractured plagioclase crystal. **D.** Cataclastic deformation of clinopyroxene and plagioclase crystals showing angular-shaped clasts formed during fracturing, grain size reduction, and grain rotation. **E.** Zone of cataclasis cutting a deformed prehnite vein. This cataclastic zone shows small rounded clasts in a clay-filled matrix.

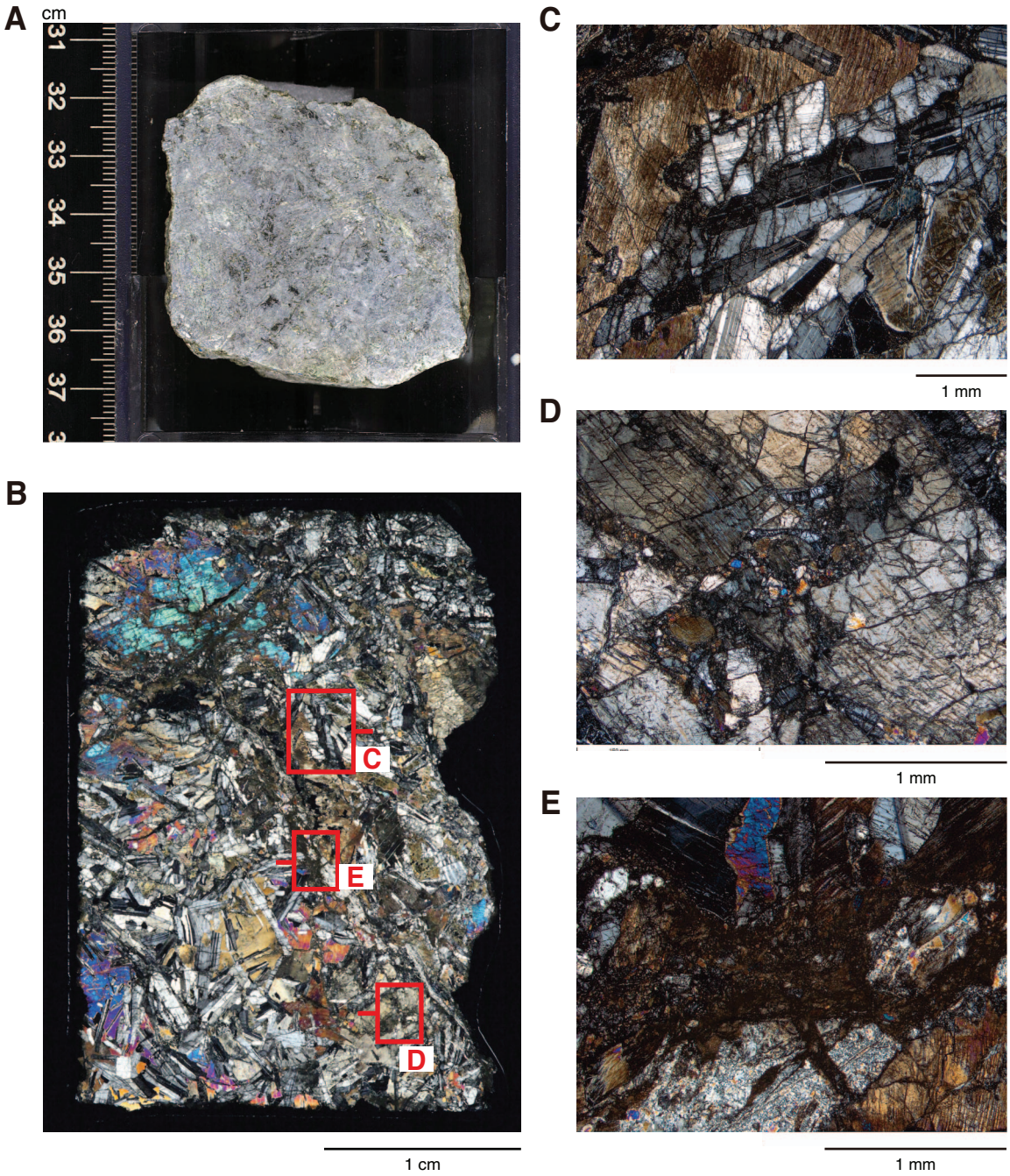

Table T1. Operations summary, Hole U1415H.

Hole U1415H (RCB coring):
Latitude: 2°15.1317′N
Longitude: 101°32.6370′W
Time at site (h): 23.4 (0445 h, 27 December–0410 h, 28 December 2012)
Seafloor (drill pipe measurement below rig floor, m DRF): 4857.6
Distance between rig floor and sea level (m): 11.2
Water depth (drill pipe measurement from sea level, mbsl): 4846.4
Total penetration (drilling depth below seafloor, m DSF): 12.9
Total depth (drill pipe measurement from rig floor, m DRF): 4870.5
Total length of cored section (m): 12.9
Total core recovered (m): 0.44
Core recovery (%): 3
Drilled interval (m): 0
Total number of cores: 1 RCB

Core	Depth (mbsf) Top of cored interval	Depth (mbsf) Bottom of cored interval	Interval cored (m)	Core recovered (m)	Curated length (m)	Recovery (%)	Date (2012)	Time UTC (h)
345-U1415H-								
1R	0.0	12.9	12.9	0.44	0.53	3	28 Dec	0420
		Total:	12.9	0.44	0.53	3		

Local ship time was UTC – 7 h. DRF = drilling depth below rig floor, DSF = drilling depth below seafloor. R = rotary core barrel (RCB) system.

Table T2. Results from X-ray diffraction analyses of cataclastic rocks, Hole U1415H.

Core, section, interval (cm)	Sample ID	ASMAN ID (file) PDF	ASMAN ID (file) Raw	ASMAN ID (file) UXD	Timestamp (UTC)	Comments	Primary phases	Secondary phases
345-U1415H-								
1R-1W, 0–2	PWDR4570261	20866341	20866351	20866331	10:05	Dark material	Chlorite	Chabazite(?)
1R-1W, 0–2	PWDR4570271	20868521	20868541	20868501	34:40	Shiny pyroxene	Clinopyroxene, thompsonite	Anorthite
1R-1W, 0–2	PWDR4570281	20868531	20868551	20868511	34:40	Zeolite-rich cataclasite	Thomsonite	Clinopyroxene, Na-anorthite
1R-1W, 0–5	OTHR4567141	20873221	20873231	20873211	45:28	Cataclastic matrix	Clinopyroxene, thompsonite	Anorthite, natrolite(?)